

An Investigation on the Effect of Particle Breakage on Rockfill Constitutive Parameters

Hossein Bazazzadeh

*Post Graduate Student, Civil Engineering Department, Hormozgan University,
Bandar Abbas, Iran
bazazzadeh.student@hormozgan.ac.ir*

Farzin Kalantary

*Assistant Professor, Civil Engineering Department, K.N.Toosi University of
Technology, Tehran, Iran
fz_kalantary@kntu.ac.ir*

Adel Asakereh

*Assistant Professor, Civil Engineering Department, Hormozgan University,
Bandar Abbas, Iran
asakereh@hormozgan.ac.ir*

ABSTRACT

Crushed rocks are being used ever more extensively in practice due to its versatility, capacity to absorb seismic energy, and adaptability to various foundation conditions. Particle breakage is an important factor influencing rockfill behavior even under low confining pressures. The breakage is expressed quantitatively by the breakage factor, B_g . The value of B_g is calculated from the sieve analysis of rockfill samples before and after triaxial tests. In the present study, the results of large drained triaxial tests and Los Angeles abrasion tests on rounded and angular rockfill materials from five different dam sites have been analysed. The stress-strain and volume change behavior of rockfill materials have also been compared against particle breakage factor. Based on the results of this investigation, the most significant parameters influencing particle breakage are found to be the inherent strength of particles, grading and state of confining pressure. Angle of friction and dilation angle are also influenced by particle breakage and other factors which intensify the breakage. It has been noted that both friction angle and dilation angle decrease with increase of particle breakage.

KEYWORDS: Rockfills, breakage, triaxial test, Los Angeles abrasion test.

INTRODUCTION

Rockfill dams are increasingly used for purposes such as irrigation, power generation, and flood control. Rockfill dams are constructed using mostly quarried rockfill materials obtained by blasting rock. In some cases such as Sahand embankment dam in Iran, alluvial rockfill materials collected from the riverbeds are used in the construction of rockfill dams. The blasted material consists of angular and subangular particles, but the alluvial (riverbed) material consists of

subrounded and rounded particles. The maximum size of rockfill materials is very large and may exceed over 1 m in certain cases.

During the past decades, great efforts have been made to study the shear behavior of rockfill materials, due to its importance to both safe and economic design of embankments and dams. Such investigation was usually carried out in large-scale triaxial testing apparatus, which have revealed that rockfills exhibit a non-linear stress-strain relationship, stress-dependence of stiffness and a non-linear strength envelope, as well as intense shearing contraction and dilatancy (Indraratna et al. 1993). Particle breakage is one of the most important factors influencing rockfill behavior and variation of constitutive parameters such as angle of friction and dilation. Particle breakage induced behaviors of rockfill materials and it has made the behavior pattern of these materials unpredictable using well-known criteria in granular soils.

This paper deals with the results of large triaxial tests and Los Angeles abrasion tests on rounded and angular rockfill materials collected from five dam sites in Iran. The focus of this study has been made on the effect of particle breakage on the stress-strain and volume change behaviors and constitutive parameters of rockfill materials. The article is organized in the following sections. Next section summarizes the background of research studies on behavior of rockfill materials. Then in third section the details of materials and testing program are presented. Results of laboratory tests are given in fourth section. Analysis of stress-strain and volume change behavior of materials and changing of constitutive parameters are discussed in fifth and sixth sections respectively.

REVIEW

Rockfill materials contain particles of large size, and testing of such rockfill materials would require equipment of formidable dimensions. Therefore, the sizes of the rockfill materials for testing are reduced by using modeling techniques. Four modeling techniques are used to reduce the size of the rockfill material. They are the scalping technique (Zeller and Wullimann 1957), parallel gradation technique (Lowe 1964), generation of quadratic size distribution curve (Fumagalli 1969), and replacement technique (Frost 1973). Ramamurthy and Gupta (1986) considered the parallel gradation method more appropriate.

Triaxial tests have been conducted on rock fragments and rockfill materials using large size triaxial testing equipment (Hall and Gordon 1963; Marsal 1967; Fumagalli 1969; Marachi et al. 1972; Thiers and Donovan 1981; Ansari and Chandra 1986; Venkatachalam 1993; Gupta 2000; Varadarajan et al. 2003; 2006). Specimen diameters in these tests ranged from 15.2 to 500 mm and maximum size of particles ranged from 3.8 to 100 mm. The materials consisted of rock fragments, blasted rockfill materials and alluvial rockfill materials from various sites. They have concluded that (1) the stress-strain behavior of the rockfill materials is nonlinear, inelastic and stress dependent, (2) an increase in confining pressure tends to increase the value of peak deviator stress, axial strain, and volumetric strain at failure, (3) an increase in the size of the particles results in an increase in volumetric strain at the same confining pressure and (4) the particle breakage increases with the size of the particles and the confining pressure. They found that the behavior of the rockfill depends on mineral composition, grain size, shape, gradation, and relative density of the rockfill.

Quantification of particle breakage

Prior to investigating of the particle degradation effect on the constitutive parameters, it is essential to identify and employ a suitable parameter that will represent the degree of particle breakage during shear deformation. In this regard, several techniques have been proposed by various investigators. In most of these methods, different empirical indices or parameters are used as indicators of particle breakage. All breakage indices are based on changes in particle sizes due to stress changes. Some indices are based on the change of a single particle size, and others are based on the change in overall grain-size distribution of aggregates. Lade et al. (1996) have discussed some of the widely used breakage indices as a form of comparison.

Marsal (1967) and Lee and Farhoomand (1967) were the first among others who developed independent techniques and indices to quantify particle breakage. Marsal noticed a significant amount of particle breakage during large-scale triaxial tests on rockfill materials and developed an index of particle breakage (B_g). His method involves the change in overall grain-size distribution of aggregates before and after the testing. From the change in grain-size distributions, the difference in percent retained on each sieve size is computed as:

$$\Delta W_k = \Delta W_{k_i} - \Delta W_{k_f} \quad (1)$$

Where ΔW_{k_i} represents the percent retained on sieve size k before the test and ΔW_{k_f} is the percent retained on the same sieve size after the test. Marsal's breakage index B_g is the sum of the positive values of ΔW_k , expressed as a percentage:

$$B_g = \sum \Delta W_k \quad (2)$$

The index B_g has a lower limit of zero, indicating no particle breakage, and a theoretical upper limit of unity (100%), representing all particles broken to sizes below the smallest sieve size used.

Lee and Farhoomand (1967) quantified the extent of particle breakage while investigating earth dam filter materials. They concentrated their study on the effects of particle crushing on plugging of dam filters and proposed a breakage factor expressing the change in a single particle size (15% passing, D_{15}), which is a key parameter in filter design, as:

$$B_g = \frac{D_{15_i}}{D_{15_f}} \quad (3)$$

Where D_{15_i} and D_{15_f} represent the particles size before and after the test respectively. Hardin (1985) defined two different quantities, namely the breakage potential B_p , and the total breakage B_t , based on the changes in grain-size distribution, and then introduced an index of particle breakage as the relative breakage B_r ($= B_t/B_p$). Hardin's method requires a planimeter or numerical integration technique for computing B_t and B_p . Miura and O-hara (1979) employed the

change in surface area (ΔS) of aggregates as the measure of particle breakage. They considered that new surfaces would be generated as the particles are broken, and therefore the change in surface area could be used as an indicator of particle breakage. In their method, several assumptions are necessary in relation to the specific surface area of different particle (sieve) sizes. Considering various methods of particle breakage quantification, Marsal's (1967) breakage index B_g has been adopted in this study because of its simplicity in computation and ability to provide a perception on the degree of particle degradation in a quantifiable manner.

Deliberation of constitutive parameters

In this study, the effects of particle breakage on two constitutive parameters, internal angle of frictional and dilatancy angle, are probed.

Dilatancy may be described as the change in volume that is associated with shear distortion of an element in the material. A suitable parameter for characterizing a dilatant material is the dilatancy angle, ψ . This angle was introduced by Hansen (1958) and represents the ratio of plastic volume change over plastic shear strain (Vermeer et al. 1984) as:

$$\tan\psi = \frac{d\varepsilon_v^p}{d\varepsilon_d^p} \quad (4)$$

The volumetric strain is calculated as:

$$\varepsilon_v = \varepsilon_a + 2\varepsilon_r \quad (5)$$

Where ε_a represent axial strain and ε_r is lateral strain. In order to obtain volumetric plastic strain, ε_v^p , by assuming sample homogeneity, the value of lateral plastic strain was considered proportional to axial plastic strain. Therefore the lateral plastic strain represent as:

$$2\varepsilon_r^p = \frac{\varepsilon_a^p}{\varepsilon_a} (\varepsilon_v - \varepsilon_a) \quad (6)$$

Finally, the volumetric plastic strain and plastic shear strain are as:

$$\varepsilon_v^p = \varepsilon_a^p + 2\varepsilon_r^p \quad (7)$$

$$\varepsilon_d^p = \varepsilon_a^p - \varepsilon_r^p \quad (8)$$

Based on equations (4) to (8), the angle of dilation is represented as:

$$\psi = \tan^{-1} \left[-\frac{2d\varepsilon_v^p}{3d\varepsilon_a^p - d\varepsilon_v^p} \right] \quad (9)$$

Frequently, separation of elastic and plastic components of strain is not straightforward, and total strain increments are used in calculation of dilative angle. For many situations, the contribution of elastic strains to total strains may be negligible when yielding is occurring, and the difference between a plastic strain increment ratio and a total strain increment ratio may be small (Wood 1990).

In order to calculate internal frictional angle, below equation was used:

$$\phi = \sin^{-1} \left[\frac{\sigma_1 - \sigma_3}{\sigma_1 + \sigma_3} \right] \quad (10)$$

Where ϕ is angle of friction and σ_1 and σ_3 are major and minor principal stress respectively.

LABORATORY TESTS

In this investigation, the results of experimental study of Sadeghpour (1998) that was done in Building and Housing Research Centre (BHRC) laboratory, Tehran, Iran, were used.

Rockfill Material Properties

The materials used in this study have been prepared from rockfill borrow areas of Aydoghmoosh, Yamchi, Vanyar, Sabalan and Sahand dams which were constructed in North West of Iran. Three type of material were quarried rockfill consisting of angular particles, while the other set were alluvial rockfill consisting of rounded to subrounded particles. The alluvial material was derived from Upper bedrock by soil drifting and quarried material was obtained by blasting. From the geology point of view, the rocks comprising the rockfill materials are andesite, diorite, dacite and basalt which are igneous origin. The details of the projects and the type of rock materials are given in Table 1.

Table 1: Location and Lithology of Rockfill Materials Used

Project name	Location	Rockfill source	Name of the rock
Aydoghmoosh dam	East Azarbayjan state, Iran	Blasting	Andesite
Yamchi dam	Ardabil state, Iran	Alluvium	Andesite and Basalt
Vanyar dam	East Azarbayjan state, Iran	Blasting	Diabase
Sabalan dam	Ardabil state, Iran	Blasting	Diorite and Andesite
Sahand dam	East Azarbayjan state, Iran	Alluvium	Diorite and Dacite

The particles of the materials were subjected to Los Angeles abrasion tests which the results and other properties of material are presented in Table 2. These values show that rockfill particles from the Aydoghmoosh site were stronger than other materials and Sahand site has weakest material.

Table 2: Properties of Rockfill Materials Used

Material name	Particle shape	Los Angeles abrasion (%)	D_{50} (mm)	C_c	C_u
Aydoghmoosh-well graded	Angular/subangular	19	7.1	2.9	25
Aydoghmoosh-poorly graded	Angular/subangular	19	3.1	0.9	3
Yamchi	Rounded/subrounded	32.5	2.5	0.7	20
Vanyar	Angular/subangular	30	7.5	2.2	25.8
Sabalan	Angular/subangular	28	6.5	2.2	22.5
Sahand	Rounded/subrounded	46.25	2.4	0.4	14.3

Since rockfill materials contained large size particles, modeled rockfill materials with maximum size of particles 50 mm, which were obtained using parallel gradation technique, are used for triaxial testing. For instance, in Figure 1 prototype and modeled rockfill material gradation for Sabalan dam will be presented. The grain size distribution curves of the modeled rockfill materials are shown in Figure 2.

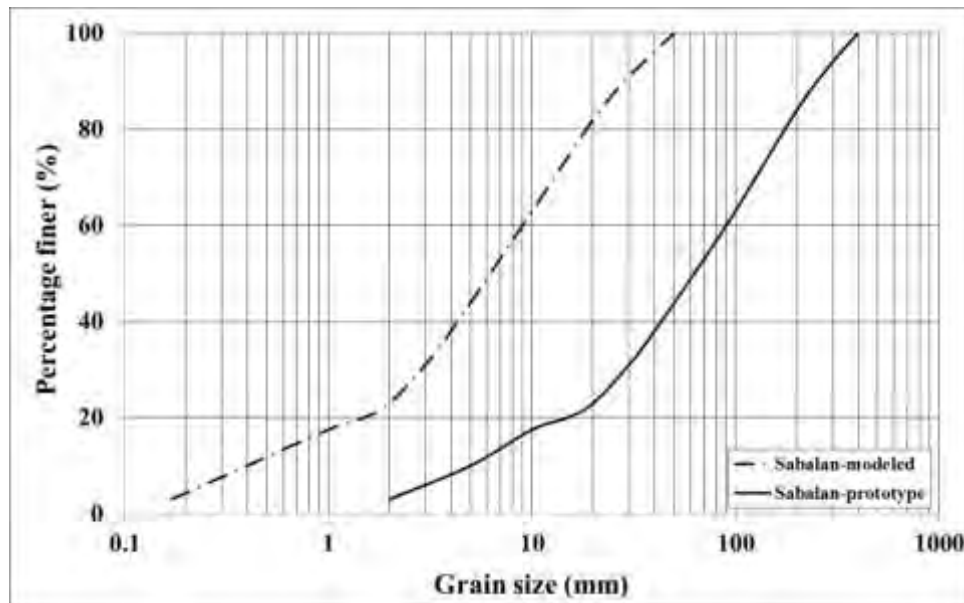


Figure 1: Grain size distribution curves for prototype and modeled sabalan rockfill

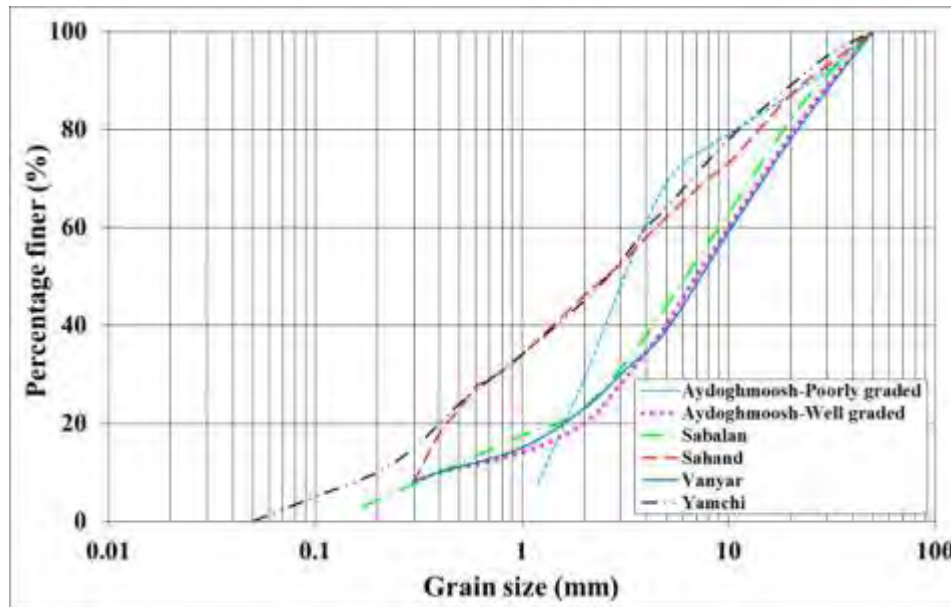


Figure 2: Grain size distribution modeled rockfill materials

Experimental procedure

A large-scale triaxial apparatus, which can accommodate specimens 300 mm diameter and 600 mm high, was used for investigating the stress-strain-volume change behavior of the modeled rockfill materials. All the measurement devices were digital and the receiver data unit was computerized. The maximum confining pressure that can be used was 20 kg/cm^2 . Further details of the equipment are given in.

For testing, the samples were prepared by compacting the materials in several equal layers by vibratory compaction in a split mold. A dry density corresponding to 95% of relative density was adopted. After placing the compacted specimen inside the triaxial cell, the cell was subjected to the suction and then the specimen was saturated. Consolidation of the specimen was commenced after achieving the pore pressure parameter, $B > 95\%$. Three confining pressures in the range between 1 and 9 kg/cm^2 were used for each modeled rockfill material. The sample was first subjected to the required consolidation pressure and then sheared to failure with a rate of loading of 0.5 mm/min . From the tests stress-strain-volume change behavior were plotted.

TEST RESULTS

Stress-strain and volume change relationships for the alluvial and quarried modeled materials with maximum size of particle of 50 mm at the confining pressures between 0.1 to 0.9 MPa are shown in Figure 3 and 4 respectively. The values of axial and volumetric strains at failure are given in Table 3.

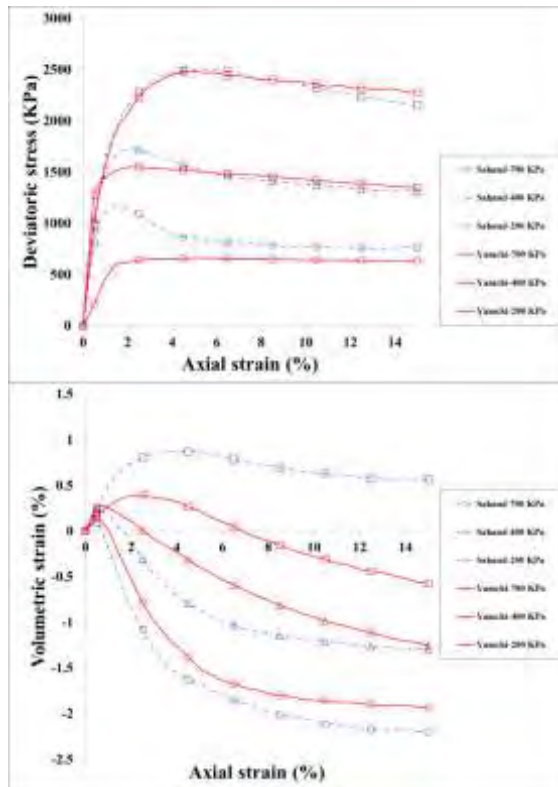


Figure 3: Stress-strain-volume change relationship for alluvial rockfill materials

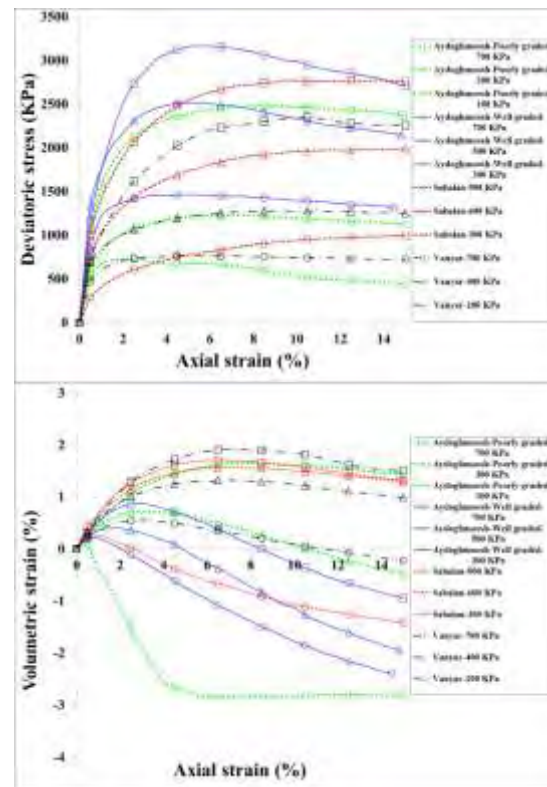


Figure 4: Stress-strain-volume change relationship for quarried rockfill material

Particle breakage was observed during shearing. As mentioned above, the breakage is expressed quantitatively by the Marsal's breakage factor, B_g . Before testing, the sample is sieved using a set of standard sieves (80 to 0.075 mm in size) and the percentage of particles retained in each sieve is calculated. After testing, the sample is again sieved and the percentage of particles retained is calculated. Due to the breakage of particles, the percentage of particles retained in large size sieves will decrease and the percentage of particles retained in small size sieves will increase. The sum of decreases in the percentage retained will be equal to the sum of increases in the percentage retained. The sum of decreases (or increases) is the value of the breakage factor. The values of B_g for the modeled rockfill materials were presented in Table 3.

Table 3: Strain at the failure in triaxial tests

Material name	Confining pressure (kPa)	Axial strain at failure (%)	Volumetric strain at failure (%)	B_g (%)
Aydoghmoosh-well graded	700	5.64	0.53	4
	500	4.41	0.08	3
	300	4.93	-0.71	2
Aydoghmoosh-poorly graded	700	7.2	1.64	4.92
	300	7.16	0.42	2.83
	100	2.44	-1.45	2.18
Sabalan dam	900	8.94	1.63	13.5
	600	7.77	1.56	7
	300	5.96	-0.6	5
Vanyar dam	700	10.66	1.79	8
	400	9.38	1.26	5
	200	4.36	0.5	3.41
Sahand dam	700	5.21	0.85	3.7
	400	1.90	-0.1	1.6
	200	1.54	-0.55	0.12
Yamchi dam	700	5.30	0.19	2.4
	400	2.13	0.076	1
	200	5.18	-1.52	0.61

INTERPRETATION AND ANALYSIS OF THE RESULTS

Quarried Rockfill Materials

Aggregates of Aydoghmoosh made of Andesite with 19% Los Angeles abrasion are stronger than aggregates of Sabalan made of Diorite and Andesite with 28% abrasion and those of Vanyar made of Diabase with 30% abrasion. Aydoghmoosh materials have failed with less deformation in comparison with other angular samples. This topic has been shown in Figure 6. Likewise, as it is shown in Figure 7, the percentage of breakage for Aydoghmoosh materials was less than other angular materials. Generally speaking, it can be seen that materials with high abrasion strength have less breakage and these materials will be ruptured in lower failure strains.

As shown in volume change behavior of angular materials in Figure 4, all samples of Aydoghmoosh materials have increasing volume, but other materials in high confining pressure have decreasing volume. This matter is because of high strength of Aydoghmoosh materials that cause lower breakage aggregates and sliding particles around them and these will result in increasing volume; however, materials with lower strength will be broken and compacted at high load service.

Increasing the confining pressure in angular materials will make high strains fail (Figure 5). Besides, softer materials will be ruptured in high strain because of the breakage discussed earlier.

Although breakage will decrease the shear strength in rockfill materials, increasing the deformation while rapturing will be considered a positive point.

Having considered poorly graded Aydoghmoosh materials and the well graded ones, we observed that the failure strains in the poorly graded samples at high confining pressure were further than the well graded ones. The mentioned difference has been revealed in Figure 5.

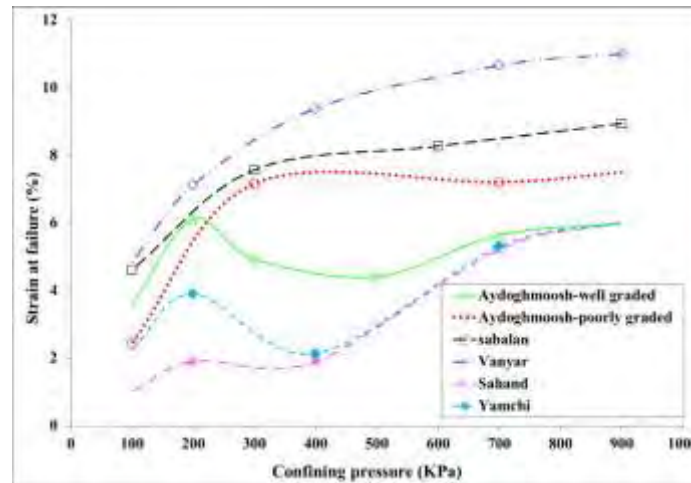


Figure 5: Variation of failure strain with confining pressure

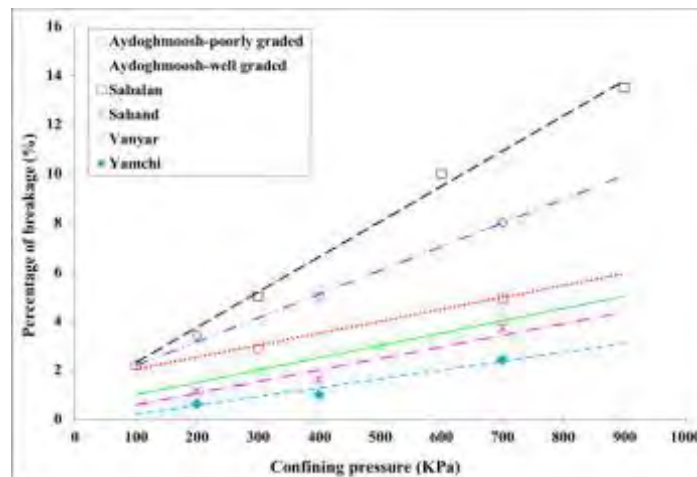


Figure 6: Variation of breakage factor with confining pressure

Alluvial Rockfill Materials

Based on Los Angeles test results, Yamchi materials with 32% abrasion have greater strength rather than Sahand aggregates with 46% abrasion. But as shown in Figure 3, Yamchi materials have high shear strength in comparison with Sahand materials at confining pressure of 200 KPa

and 400 KPa. Also in the same conditions, Sahand materials failed at more axial strain than Yamchi materials.

Based on these results, it can be understood that the load capacity of riverbed rounded rockfill materials have no direct relationship with the abrasion strength. So in order to compare the behavior and peak of load service of rockfill masses, no one can think of determining of rockfill materials abrasion strength as an appropriate tool. As shown in Figure 2, the percentage of finer particles than 5 mm for Yamchi and Sahand materials were respectively 65% and 62%. Likewise, percentage finer than 0.3 mm in Yamchi and Sahand materials are respectively 15% and 8%. Based on this point that the conditions of samples in moisture, compaction, confining pressure, particle shape and type of rock are approximately equal, it can be realized that deference between strength of these samples refers to the finer materials.

STUDY OF CONSTITUTIVE PARAMETERS

In this section, variation of frictional angle and angle of dilation against different test condition are probed. These constitutive parameters were calculated based on equations (9) and (10). For each test, the dilation angle at failure and the maximum of frictional angle are considered as value of these constitutive parameters.

Internal Frictional Angle

Comparing of rockfill materials frictional angles by various criterions that are shown in Figure 7, indicates that many of these materials have greater shear strength rather than average strength of rockfill materials. The angle of shear resistance vs. confining pressure for the rockfill materials are shown in Figure 8.

The angle of shear resistance decreases as long as the confining pressure for these materials is going up. In the meantime, the opposite trend is observed for the breakage factor. As the confining pressure increases in a granular material, lower void ratio, which provides greater interlocking, is achieved for the same compactive effort. But a greater degree of particles breakage also occurs when the larger confining pressure is witnessed, and this phenomenon dates back to the greater force per contact (Lambe and Whitman 1969). The effect of the increase in interlocking is to increase the shear resistance, while the particles breakage effects leads to its reduction. The net effects of these factors will cause the reduction in the angle of shear resistance with confining pressure.

As shown in Figure 8, the angle of shear resistance regarding poorly graded Aydoghmoosh materials is less than that of well graded Aydoghmoosh materials. The reason of this matter is the greater interface between aggregates for well graded materials that cause low stress in each contact of particles. For poorly graded materials, because of the paucity of particles with average size, stress in aggregates contacts will increase. Consequently, the particles breakage will go up and it will result in the reduction of the shear resistance angle.

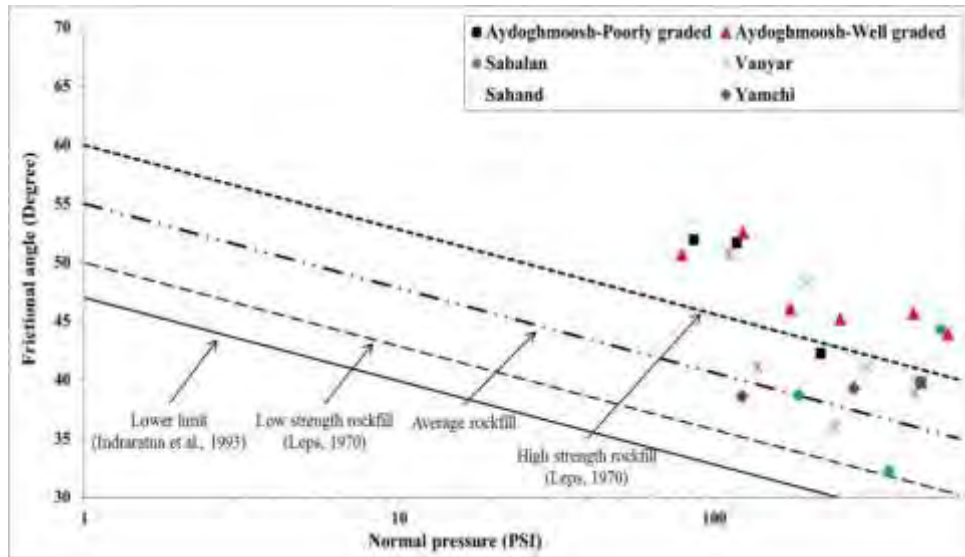


Figure 7: Comparing of frictional angle against various criterions

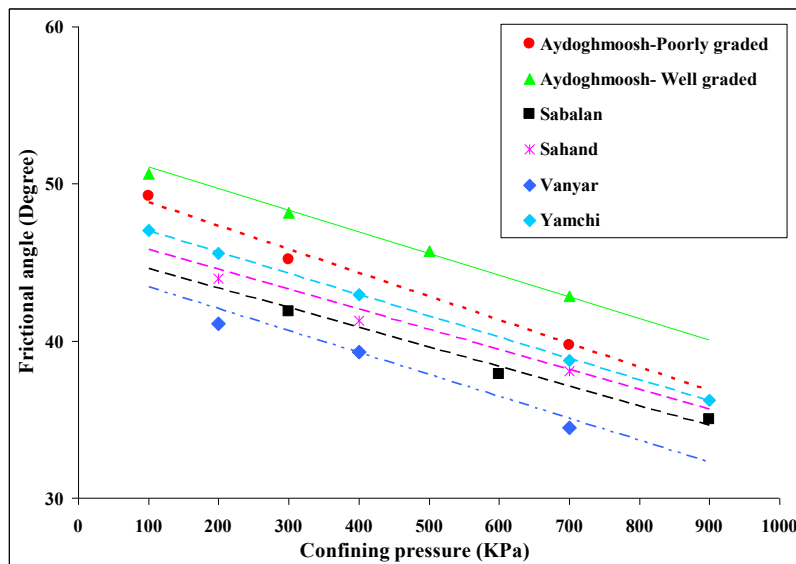


Figure 8: Variation of frictional angle against confining pressure

By used of stress ratio $\beta_f = ((\sigma_1 - \sigma_3)/(2\sigma_3))_f$, variation of peak angle of friction against this ratio will be logarithmic. For instance, the diagram of this variation for Aydoghmoosh materials is shown in Figure 9. The equations of these logarithmic curves for Aydoghmoosh, Vanyar and Sahand materials, that had well fitted, are presented in Table 4.

Jalali (1988) in his investigation presented below equations for Basalt and Asmary limestone materials respectively:

$$\varphi_p = 38.81 \operatorname{Log} \left(\frac{\sigma_1 - \sigma_3}{2\sigma_3} \right)_f + 30 \quad (11)$$

$$\varphi_p = 39.21 \operatorname{Log} \left(\frac{\sigma_1 - \sigma_3}{2\sigma_3} \right)_f + 30 \quad (12)$$

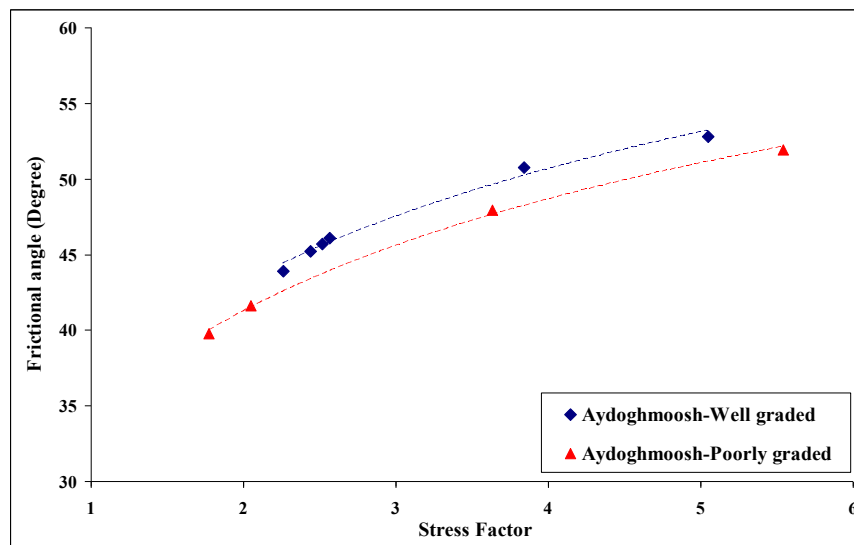


Figure 9: Variation of frictional angle against stress factor

Table 4: Relation between principal stress at failure and frictional angle

Equation	Material type
$\varphi_{(Degree)} = 25.33 \operatorname{Log} \left(\frac{\sigma_1 - \sigma_3}{2\sigma_3} \right)_f + 35.86$	Aydoghmoosh-Well graded
$\varphi_{(Degree)} = 26.42 \operatorname{Log} \left(\frac{\sigma_1 - \sigma_3}{2\sigma_3} \right)_f + 34.18$	Aydoghmoosh-Poorly graded
$\varphi_{(Degree)} = 41.96 \operatorname{Log} \left(\frac{\sigma_1 - \sigma_3}{2\sigma_3} \right)_f + 28.68$	Vanyar
$\varphi_{(Degree)} = 40.53 \operatorname{Log} \left(\frac{\sigma_1 - \sigma_3}{2\sigma_3} \right)_f + 28.95$	Sahand

As can be shown, the equations of Table 4 are consistent with above equations.

Dilation Angle

By increasing the confining pressure, the range of dilation angles will decrease. This matter has been shown in Figure. 10. In low confining pressure, based on the gradation, density, the type of the rock and the particles shape, dilation angles will change in wider range. Breakage of particles causes changing the gradation of materials. Therefore, it has high effects on the dilation behavior of rockfill materials. As the confining pressure increases, the value of breakage factor will go up and the dilation angle will decrease.

Regarding the Aydoghmoosh materials, the percentage of particles finer than 5 mm for well graded and poorly graded samples are 41% and 69% respectively. On the other hand, D_{50} for well graded and poorly graded of Aydoghmoosh materials are 7.1 and 3.1 mm respectively. So based on the greater value of D_{50} for well graded materials, it will be expected that the contact stress will be high and the particles breakage will increase and as a result, dilation angle will lower than those of poorly graded materials. But because of uniformity of poorly graded materials, as shown in Figure 10, the dilation angle will be less in these materials.

The results of some researches indicate that the angle of shear resistance for coarse grained material with 30% to 40% particles finer than 5 mm, is five degree greater than materials which lack the mentioned finer materials. Also granular materials with 30% to 40% aggregate finer than 5 mm, have approximately double bulk modules rather than materials without the mentioned finer ones. In general, the rockfill materials with 30% to 40% fine materials, have appropriate strength and flexibility (Vutsel 1983).

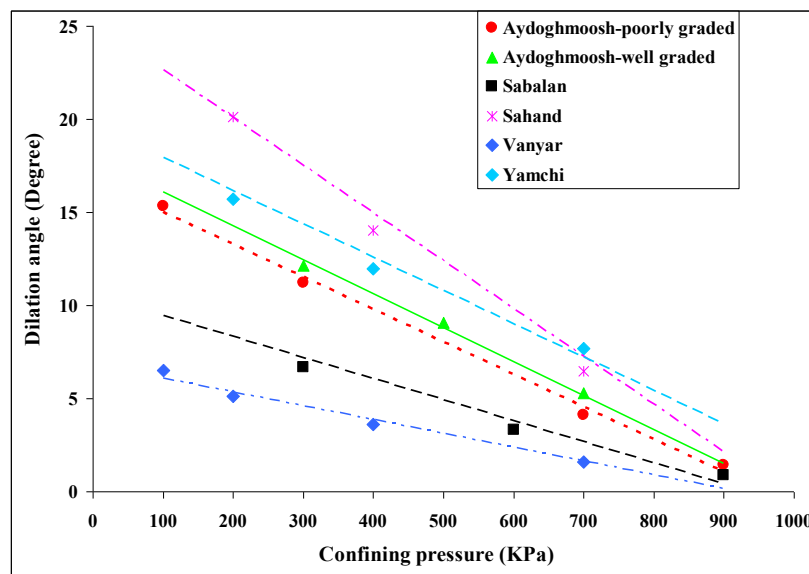


Figure 10: Variation of dilation angle with confining pressure

The analysis of dilation angles for rounded rockfill materials indicates that Sahand materials have greater value of dilation rather than Yamchi materials at 200 and 400 KPa confining pressure. But at 700 KPa confining pressure, dilation in Yamchi materials is greater than Sahand

materials. So it can be seen that in rounded rockfill materials, at high confining pressure, because of the breakage effect, the dilation angle change was affected by abrasion strength.

The variations of axial strain for peak of dilation angle against confining pressures are presented at Figure 11. As it is shown, for greater confining pressures, greater axial strains are required to provide maximum dilation. This matter result of high material compaction because of high confining pressures that cause be required great energy for create volume expansion.

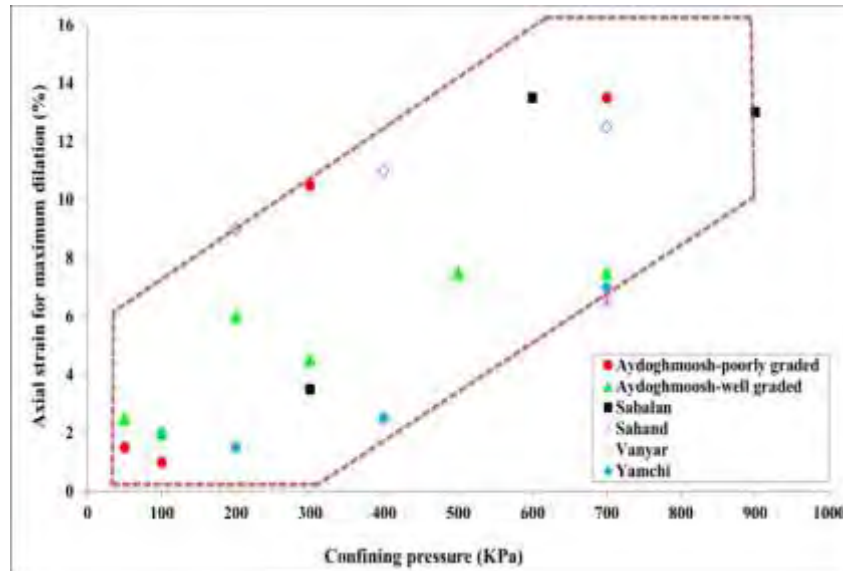


Figure 11: Axial strain for maximum dilation against confining pressure

CONCLUSION

In this study, different tests have been conducted on rockfill materials taken from five large dams located in North West of Iran. The results obtained from this study are summarized as follows:

- 1- Regarding the quarried and alluvial rockfill materials, it seems that materials with high abrasion strength have less breakage and these materials are ruptured in low failure strain.
- 2- During the shearing at high confining pressure in quarried materials, the samples with high abrasion strength, because of low breakage aggregates and sliding particles around them, have increasing volume, but other materials, due to high breakage and compacting, have decreasing volume.
- 3- In these rockfill materials with increasing confining pressure, failures are done in high strain.
- 4- The failure strain in poorly graded materials are more than well graded ones at high confining pressure because of increasing the particle breakage in uniform materials.
- 5- Based on results of alluvial materials, it can be understood that the load capacity of riverbed rockfill materials has no direct relationship with abrasion strength. According to this investigation, the deference between strength of these samples refers to finer materials.
- 6- The angle of shear resistance decreases with the confining pressure as long as the opposite trend is being observed for the breakage factor.
- 7- Angle of shear resistance for poorly graded materials at high confining pressure is less than that of well graded materials.
- 8- By increasing the confining pressure, the value of breakage factor will increase and the dilation angle will decrease.
- 9- The rockfill materials with 30% to 40% fine materials have appropriate strength and flexibility.

REFERENCES

1. Ansari, K. S., and Chandra, S. (1986). "How ought one to determine soil parameters to be used in the design of earth and rockfill dams." Proc., Indian Geotechnical Conf., New Delhi, India, 2, 1–6.
2. Frost, R. J. (1973). "Some testing experiences and characteristics of boulder-gravel fills in earth dams." ASTM, STP, 523,207.
3. Fumagalli, E. (1969). "Tests on cohesionless materials for rockfill dams." J. SMFE, ASCE, 95 (SM1), 313–332.
4. Gupta, A. K. (2000). "Constitutive modeling of rockfill materials." PhD thesis, Indian Institute of Technology, Delhi, India.

5. Hall, E. B., and Gordon, B. B. (1963). "Triaxial testing using large scale high pressure equipment." STP 361, ASTM, Philadelphia, 315–328.
6. Hardin, B.O. (1985). "Crushing of soil particles." *Journal of Geotechnical Engineering, ASCE*, 111(10): 1177–1192.
7. Inderaranta, B., Wijewardena, L. S. S., and Balasubramaniam, A. S. (1993), "Large-scale triaxial testing of greywacke rockfill" *Geotechnique*, London, U. K., 43(1), 37-51.
8. Indraratna, B., Wijewardena, L. S. S., Balasubramaniam, A. S., (1993). "Large-scale triaxial testing of greywacke rockfill." *Geotechnique*, 43(1), 37–51.
9. Jalali, H., (1988). "Mechanical properties of crushed rocks." *International of dam construction*, Tehran, Iran.
10. Lade, P.V., Yamamuro, J.A., and Bopp, P.A. (1996). "Significance of particle crushing in granular materials." *Journal of Geotechnical Engineering, ASCE*, 122(4): 309–316.
11. Lambe, T. W., and Whitman, R. V. (1969). *Soil mechanics*, Wiley, New York.
12. Lee, K.L., and Farhoomand, I. (1967). "Compressibility and crushing of granular soil in anisotropic triaxial compression." *Canadian Geotechnical Journal*, 4: 69–86.
13. Leps, M. Thomas., (1970). "Review of shearing strength of rockfill," *Journal of the Soil Mechanics and Foundations Division, ASCE*, Vol. 96, pp. 1159 – 1170.
14. Lowe, J. (1964). "Shear strength of coarse embankment dam materials." *Proc., 8th Int. Congress on Large Dams*, 3, 745–761.
15. Marachi, N. D., Chan, C. K., and Seed, H. B. (1972). "Evaluation of properties of rockfill materials." *J. SMFE*, 98(1), 95–114.
16. Marsal, R. J. (1967). "Large scale testing of rockfill materials." *J. SMFE, ASCE*, 93(2), 27–43.
17. Miura, N., and O-hara, S. (1979). "Particle crushing of decomposed granite soil under shear stresses." *Soils and Foundations*, 19(3): 1–14.
18. Ramamurthy, T., and Gupta, K. K. (1986). "Response paper to how ought one to determine soil parameters to be used in the design of earth and rockfill dams." *Proc., Indian Geotechnical Conf., New Delhi, India*, 2, 15–19.
19. Sadeghpour, A. H. (1998). "Investigation of particle breakage phenomenon in materials of earth and rockfill dams" M.Sc thesis, Tarbiat modares university, Tehran, Iran.
20. Thiers, G. R., and Donovan, T. D. (1981). "Field density gradation and triaxial testing of large-size rockfill for little blue run dam." *Laboratory Shear Strength of Soil, ASTM, STP, 740*, R. N. Yong and F. C. Townsend, eds., ASTM, Philadelphia, 315–325.
21. Varadarajan A, Sharma KG, Abbas SM, Dhawan AK. (2006) "Constitutive model for rockfill materials and determination of material constants". *Int J Geomech*, 6(4), 226–37.
22. Varadarajan, A., Sharma, K. G., Venkatachalam, K., and Gupta, A. K. (2003). "Testing and modeling two rockfill materials." *J. Geotech. Geoenviron. Eng.*, 129(3), 206–218.
23. Venkatachalam, K. (1993). "Prediction of mechanical behavior of rockfill materials." PhD thesis, Indian Institute of Technology, Delhi, India.

24. Vermeer, P. A. and Brost, R., (1984), "Non-Associated plasticity for soils, concrete and rock." *Heron*, Vol. 29, No. 3, pp. 5- 23.
25. Vutsel, V. I.,(1983). "Materials for high embankment dams" *Water Power & Dam Construction*, pp 33-37.
26. Wood, D. M., (1990). "Soil behavior and critical state soil mechanics". Cambridge University Press., pp. 226-255
27. Zeller, J., and Wullimann, R. (1957). "The shear strength of the shell materials for the Go-Schenenalp Dam, Switzerland." *Proc., 4th Inst. J on SMFE, London, 2*, 399–404.

